HJR

Optimising T2 relaxation measurements on MS patients utilising a multi-component tissue mimicking phantom and different fitting algorithms in T2 calculations, p. 18-31

VOLUME 4 | ISSUE 2

ORIGINAL ARTICLE Medical Physics

Optimising T2 relaxation measurements on MS patients utilising a multi-component tissue mimicking phantom and different fitting algorithms in T2 calculations

Georgios I. Kalaitzakis[1,2], Efrosini Papadaki[2,3], Eleftherios Kavroulakis[3],
Themistoklis Boursianis[1], Konstantinos Marias[2], Thomas G. Maris[1,2]

[1]Department of Medical Physics, University of Crete, Heraklion, Crete, Greece
[2]Computational BioMedicine Laboratory,Institute of Computer Science, Foundation for Research and Technology-Hellas (FORTH), Heraklion, Crete, Greece
[3]Department of Radiology, University of Crete, Heraklion, Crete, Greece

ABSTRACT

Purpose: To evaluate the optimal regression fitting algorithm for T2 relaxation time measurements on relapsing remitting multiple sclerosis (RRMS) patients and Healthy Subjects (HS) with the aid of a multi-component tissue mimicking phantom.

Material and Methods: Twenty eight glass test tubes were filled mainly with (a) standard EUROSPIN test objects, (b) Gd-DTPA hydatic solutions, (c) milk creams with various fat contents and (d) raw eggs with various relative concentrations of egg-white and egg-yellow parts. Two patients with relapsing remitting multiple sclerosis (RRMS) and a healthy volunteer were examined. A multi-echo spin echo sequence (32 echoes) was used for all the phantom and human subjects T2 measurements. T2 relaxation parametric maps for the phantoms and the human subjects were calculated uti-

lising a Conventional-Linear (CL), a Weighted-Linear (WL), a Non-Linear (NL) and a Double-Exponential-Non-Linear-Fit (DENLF) regression fitting methods.

Results: A single T2 relaxation behaviour was observed for EUROSPIN and Gd-DTPA solution test tubes. A double T2 relaxation behaviour, revealed only by DENLF, was observed for milk creams, raw eggs, Normal-White-Matter (NWM) of a healthy subject and Normal-Appearing-White-Matter (NAWM) and focal lesions of RRMS patients.

Conclusions: WL, NL and DENLF algorithms proved to be an excellent means for optimised measurements of T2 values on tissue mimicking phantoms, NWM, NAWM and demyelinating lesions of RRMS patients. DENLF provides additional information related to differentiation of molecular environments in either phantoms or human subjects.

| CORRESPONDING AUTHOR, GUARANTOR | Georgios I. Kalaitzakis, Electrical and Computer Engineer, Medical Physics Department, University of Crete, 71201, Voutes, Heraklion, Crete, Greece, Email: giorgo.kalaitzakis@gmail.com |

Optimising T2 relaxation measurements on MS patients utilising a multi-component tissue mimicking phantom and different fitting algorithms in T2 calculations, p. 18-31

VOLUME 4 | ISSUE 2

HJR

Introduction

MRI phantoms are an important means for any MRI clinical sequence calibration experiment, considering the fact that they provide a reference standard of known parameters to be estimated. Many alternatives for the fabrication of single exponential T2 phantoms for tissue mimicking materials have been proposed but only a few choices exist for the fabrication of double/multi exponential T2 phantoms [1] that actually mimic the majority of brain and muscle tissue.

Conventional MR images can be considered, in terms of their image contrast information, as weighted entities of PD (hydrogen Proton Density), T1 (longitudinal relaxation time), T2 (transverse relaxation time), T2* (overall observed transverse relaxation time, including field inhomogeneities), water/blood molecular diffusion, water/blood molecular perfusion and macroscopic flow. The nature of any MR image contrast is practically based on the relative contributions of all the above entities at different tissues.

Quantitative MRI is a direct representation of the actual parameter obtained from the indirect contributions of all the above parameters and is presented as a 2D/3D MR image with contrast based on the relative parameter. Most commonly, the result is a 2D/3D parametric map which depicts in a gray or colour scale the measured values of the parameter in question (T2 map, T1 map, T2* map, ADC map, Perfusion map, flow map, etc). All parametric maps are obtained by appropriate mathematical fitting or algebraic calculations on the conventional MR signal data and subsequent extraction of the values of the measured parameter. In mathematical fitting, the accuracy and precision of the fitting method/algorithm is of particular importance, so that the generated parametric map is reliable and accurate [2].

Most relaxometric T2 studies which are based on T2 parametric maps are focused on mono-exponential fitting analysis methods [3]. T2 parametric maps are of vital importance when extracted from multi-exponential fitting analysis methods. These more complicated methods for the characterisation of the T2 decay curve are able to identify multiple water reservoirs in normal human brain [4-13] or characterise additional signal arising from brain white matter pathology such as demyelination or inflammatory oedema [14].

The aim of this study is to compare four different regression fitting algorithms for optimising measurements of T2 relaxation times in brain tissue mimicking phantoms and apply the best fitting algorithm in healthy subjects and relapsing remitting multiple sclerosis (RRMS) patients to validate its utility in clinical practice.

Material and Methods

2.1 Phantoms

Twenty eight test tubes filled with various materials, which simulate T2 values of different human brain physiology and pathology embedded in a plastic holder, served as a generic T2 relaxation phantom (**Tables 1, 2**). The test tubes were filled with materials which consisted of: (a) gadolinium doped agarose gel solutions as obtained from the standard EUROSPIN gel test objects (TO5) with EUROSPIN test tube vial numbers 1, 2, 3, 4, 5, 6, 7 and 8 (8 vials) [15-17]. (b) two vials containing Gd-DTPA hydatic solutions, (c) one vial containing double distilled water, (d) one vial containing Acetone, (e) eight vials containing standard milk creams with various fat contents, (f) one vial containing corn oil and (g) seven vials containing raw eggs with various relative concentrations of egg-white and egg-yellow parts. The expected range of T2 values in reference to all materials spanned from 20 ms up to 2000 ms. All test tube vials were placed in a phantom holder and their distinct positions are shown in **Table 1**. The whole construction with the embedded test tube vials is referred as the T2-QMRI phantom. The chemical composition, equivalent concentrations and labelling of all the phantom materials are presented in **Tables 1 and 2**.

2.2 Human subjects

Two patients with relapsing remitting multiple sclerosis (RRMS) (one male, 25 years, EDDS=2.5 and one female, 32 years, EDSS=3.5) and a healthy volunteer (one female, 30 years) were examined. Informed written consent as approved by the Heraklion University Hospital ethical committee, was obtained for all human subjects.

2.3 MR Image acquisition

All phantom experiments and human subjects' examinations were performed on a 1.5 T superconducting MR imager (Vision/Sonata hybrid System, Siemens, Erlangen, Gradient
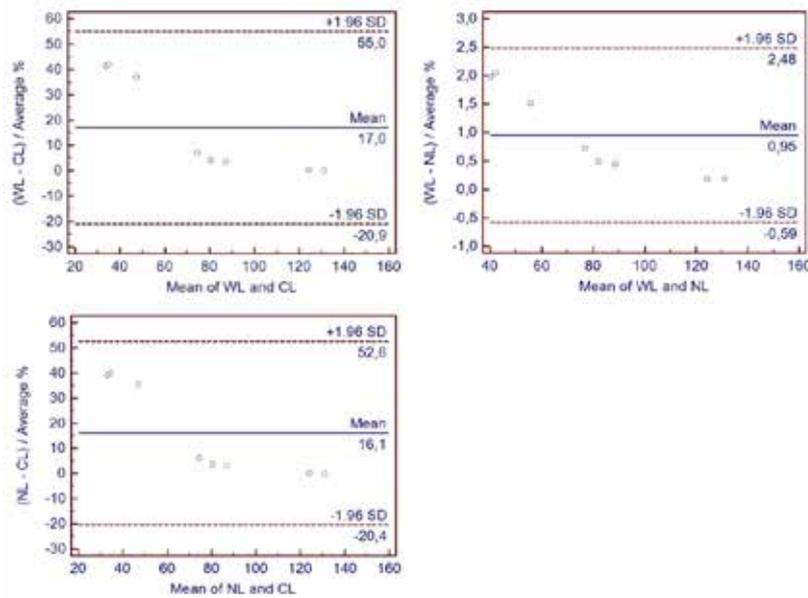
HJR

Optimising T2 relaxation measurements on MS patients utilising a multi-component tissue mimicking phantom and different fitting algorithms in T2 calculations, p. 18-31

VOLUME 4 | ISSUE 2

Fig. 1. *Bland-Altman plots for the EUROSPIN test objects.*
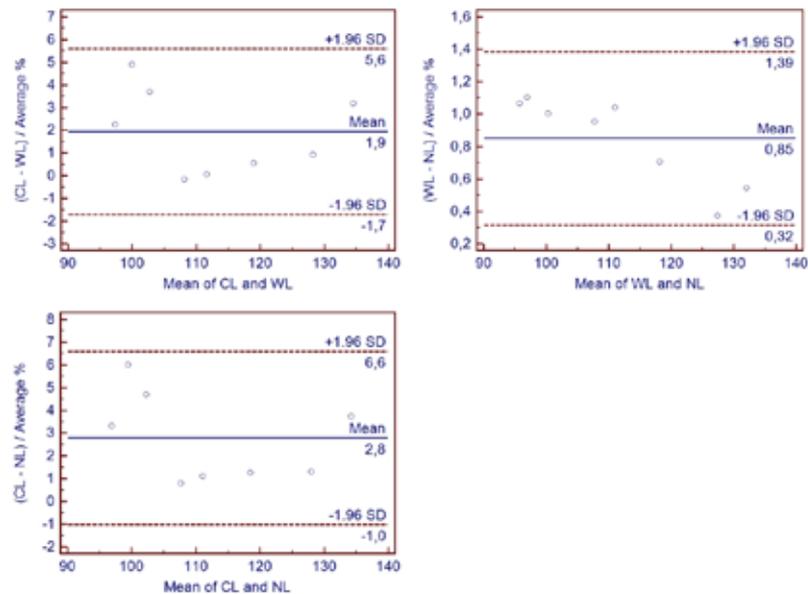

Fig. 2. *Bland-Altman plots for Milk Creams test objects.*

Strength: 45 mT m^{-1}, Slew Rate: 200 mT m^{-1} s^{-1}). A standard quadrature RF body coil was used in all examinations for signal excitation and a 4 element, 2 channel head array coil was used for signal detection. The T2-QMRI phantom was placed in supine position (test tubes facing up) and entered the magnet cradle using the head-first configuration. A conventional Gradient Echo (GRE) 2D multi slice multi plane turbo Fast Low Angle Shot (turboFLASH) T1 weighted imaging sequence was initially applied in axial, sagittal and coronal planes for the localisation of the phantom test tubes and the brain anatomical

structures of the human subjects.

For the quantitative T2 measurements, a 2DPD to T2 weighted multi-slice-Multi-Echo Spin Echo (MESE) sequence was used. This MESE sequence was based on a 2DCarr-Purcell-Meiboom-Gill (CPMG) multi-echo train sequence with alternating 180° RF pulses under the Phase-Alternating-Phase-Shift (PHAPS) scheme [18]. The MESE sequence was applied using 32 symmetrically repeated spin echoes. The first TE was 6.7 ms and the rest 31 TE's were obtained thereafter every 6.7 ms (6.7, 13.4, 20.1, 26.8...207.7, 214.4). A selective refocusing RF pulse scheme

Optimising T2 relaxation measurements on MS patients utilising a multi-component tissue mimicking phantom and different fitting algorithms in T2 calculations, p. 18-31

VOLUME 4 | ISSUE 2

HJR

was utilised. Five slices of 8 mm slice thickness and 8 mm interslice gap were used. A TR of 2300 ms was used in both phantom and human subject measurements. A field of view (FOV) image area of 280 X 210 mm^2 was covered from each slice. The image reconstruction matrix was 256 X 192 pixels respectively to the FOV dimensions, corresponding to a square pixel matrix with pixel dimensions 1.1 X 1.1 mm^2 (in-plane spatial resolution). The cross-plane spatial resolution was equal to the slice thickness (8 mm). The overall spatial resolution expressed in data voxel dimension was 1.1 X 1.1 X 8 mm^3. The total imaging dimension on the cross-plane direction (all slices and gaps) was 72 mm covering the central area of the longitudinal axes of the test tubes and most of the central cranial anatomy.

The highest possible receiver bandwidth (501 Hz/pixel) was used in order to eliminate geometric distortions due to susceptibility artefacts and also to minimise chemical shift artefacts due to fatty components. 2D geometric distortion filtering was also applied in order to eliminate geometric distortions due to inherent gradient field imperfections. The overall SNR measured on the first echo proton density weighted image of the MESE sequence was approximately 120 in both phantom experiments and human subjects' examinations. Partial Fourier imaging covering the (4/8) of k-space lines was utilised in order to keep the examination time to a minimal value. One signal average was used. The total examination time was approximately 3.5 mins.

For the implementation of phantom experiments, five coronal slices of 8 mm slice thickness and 8 mm interslice gap were used. The longer depicted anatomical axis (Head to Feet direction for the coronal slices) was always chosen as the frequency encoding axis.

For the implementation of human subjects' examinations, five oblique axial slices of 8 mm slice thickness and 8 mm interslice gap were used. The longer depicted anatomical axis (Oblique anterior to Oblique posterior direction for the axial oblique slices) was always chosen as the frequency encoding axis.

In order to avoid any off resonance excitation and magnetisation transfer effects, sequential slices were positioned far apart from each other. In both the phantom and the clinical sequences, slice gaps were equivalent to slice thicknesses. Moreover, an interleaved slice excitation scheme was also chosen in order to avoid cross talking effects (partial signal saturation) amongst the slices.

The above 2D quantitative MESE sequence, applied in both phantom and clinical T2 measurements, was meticulously designed in order to obtain the best possible accuracy in T2 measurements for short (10<T2<50) and long (60<T2<200) T2 values,

eliminate unwanted stimulated echoes and minify the effect of T1 dependence on the measurement of T2 values. This sequence was easily incorporated to the clinical protocol and was used for the final tissue double-compartment measurements of T2 relaxation times. This sequence has the ultimate advantage of being fast enough (3.5 mins) to be incorporated to any standard clinical examination protocol.

2.4 MR data handling and quantitative image analysis
Mathematical fitting algorithms
Quantitative MR data analysis was performed utilising in-house software (QMRI utilities-X) designed for this purpose by two of the authors (GK, TGM) on a separate workstation. T2 colour parametric maps were constructed on a voxel by voxel basis by fitting exponential decay curves to the signal intensities of the corrsponding voxels against TE time. T2 relaxation colour parametric maps were thus calculated utilising four different methods (a, b, c, d), each one based on different fittng algorithms.

Methods a, b, c and d are described in the following context:

a) Conventional Linear fitting method (CL):
In the Conventional Linear fitting method (CL), a standard linear fit on all logarithmic echo signal intensities of the T2 relaxation decay data is performed (QMRI Utilities-X). Proton-Density parametric maps $PD_{(x,y)}$ and T2 relaxation time parametric maps $T2_{(x,y)}$ which best fit to the experimental data were obtained by a linear mathematical fit to the equation Eq. (1) on a voxel by voxel basis(x, y):

$$S_{(x,y)}(TE) = Bg + PD_{(x,y)} \cdot exp\left(-\frac{TE}{T2_{(x,y)}}\right) \rightarrow$$

$$\ln\left[S_{(x,y)}(TE) - Bg\right] = lnPD_{(x,y)} - \frac{TE}{T2_{(x,y)}}$$

(1)

T2 relaxation decay curves were analysed assuming a mono-exponential decay behaviour in the presence of the image stack background (Bg) which is subtracted from the actual signal data. It is assumed that image noise, expressed as the SD of an artefact free background signal, is evenly distributed in all echo signals or the relative weighted images in the image stack. Each echo signal is obtained unedited without further correction.

b) Weighted Linear fitting method (WL):
In the Weighted Linear fitting method (WL), all the signal intensities were weighted prior to the standard linear fit on all logarithmic echo signal intensities of the T2 relaxation decay data [19] (QMRI Utilities-X). The T2 relaxation decay curves
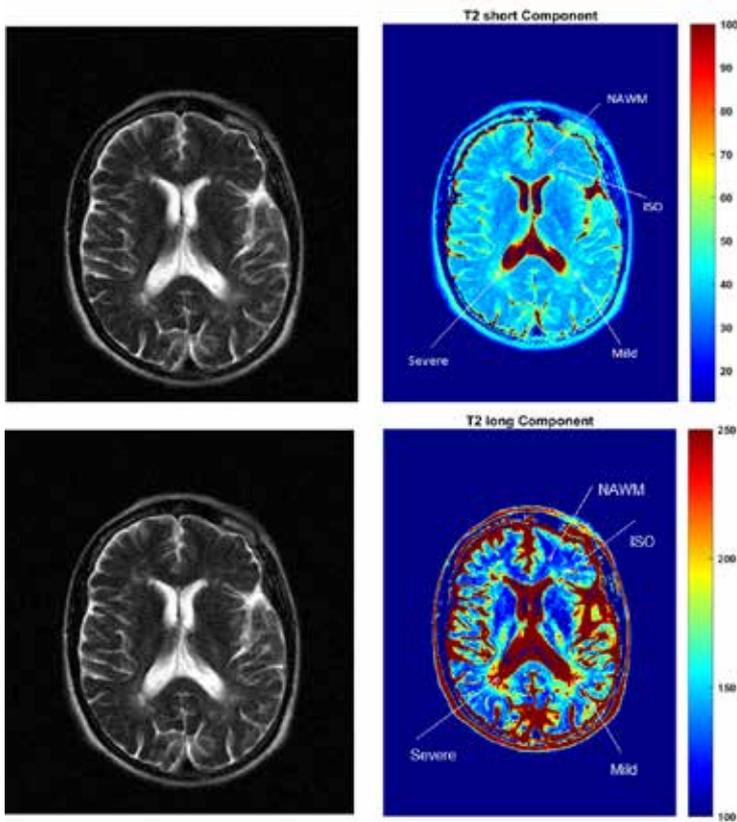
Optimising T2 relaxation measurements on MS patients utilising a multi-component tissue
mimicking phantom and different fitting algorithms in T2 calculations, p. 18-31

VOLUME 4 | ISSUE 2

Fig. 3. T2W MESE sequence for a TE of 214.4 ms (upper & down Left). Parametric T2-Short map (upper right) and parametric T2-Long map (lower right). Parametric maps created utilising DENLF method for human subject case 1. T2 decay curves related to the depicted annotations (ROIs) (upper and lower right) are presented in Fig. 7.
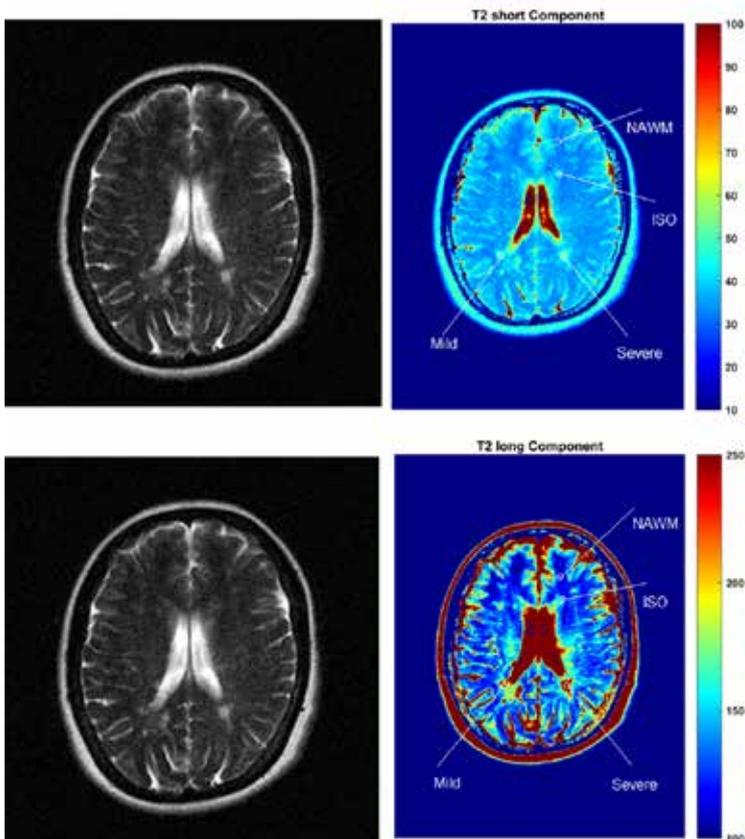
Fig. 4. T2w MESE sequence for a TE of 214.4 ms (upper & down left). Parametric T2-Short map (upper right) and parametric T2-Long map (lower right). Parametric maps created utilising DENLF method for human subject case 2. T2 decay curves related to the depicted annotations (ROIs) (upper and lower right) are presented in Fig. 8.
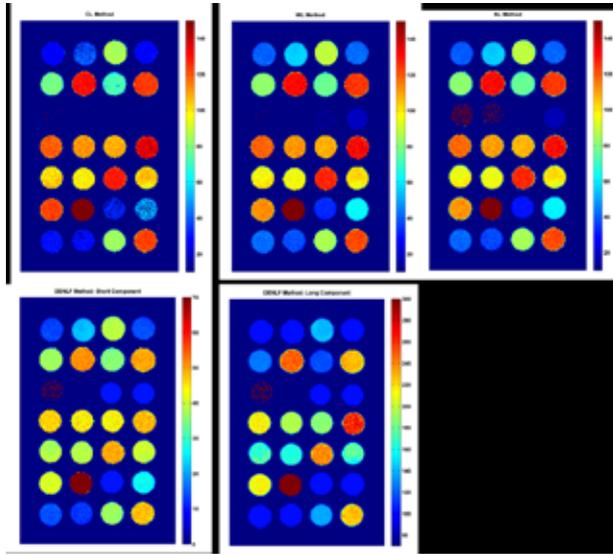
Optimising T2 relaxation measurements on MS patients utilising a multi-component tissue mimicking phantom and different fitting algorithms in T2 calculations, p. 18-31

VOLUME 4 | ISSUE 2

HJR

Fig. 5. *Colour T2 parametric maps, from different in-house fitting algorithms for the T2-QMRI phantom.*

Fig. 6. *All regression fitting algorithms for a particular pixel positioned on the milk cream tube (MC5 35%) of the T2-QMRI phantom.*

were analysed assuming a mono-exponential decay behaviour in the presence of the image stack background (Bg) which is again subtracted from the actual signal data. Each echo signal (S_i) is corrected via a specific weighting factor $S_i(w_i)$ prior to the actual weighted linear fit for the final T2 calculation. The relevant weighted factors w_i can be expressed as follows:

$$S_i(w) = w_i \cdot S_i \ , \quad w_i = \left(\frac{1}{(R_f \sigma S_{32})}\right)^2 \qquad (2)$$

Finally, the logarithmic transformation of the actual data (y_i) prior to the final fit reveals the following formulas for y_i, σy_i, w_i and $y_i(w)$:

$$y_i = \ln(S_i - Bg) \ , \qquad \sigma y_i = \frac{\sqrt{2} \cdot R_f \cdot \sigma S_{32}}{S_i}, \qquad w_i = \frac{S_i^{\ 2}}{2(R_f \cdot \sigma S_{32})^2}$$

$$y_i(w) = w_i \cdot y_i \leftrightarrow y_i(w) = \frac{S_i^{\ 2}}{2(R_f \cdot \sigma S_{32})^2} \cdot y_i \qquad (3)$$

It is clearly seen that due to the calculated weight factor from equation Eq. (3), weighting is proportional to the actual signal value. Higher signal values have significant weights on the weighted linear fit and more significant contribution for the final T2 calculations. Proton-Density parametric maps $PD_{(x, y)}$ and T2 relaxation time parametric maps $T2_{(x, y)}$, which best fit to the experimental weighted data were calculated by a weighted linear mathematical fit to the equation Eq. (4) on a voxel by voxel basis $_{(x, y)}$:

$$Sw_{(x,y)}(TE) = Bg + PD_{(x,y)} \cdot exp\left(-\frac{TE}{T2_{(x,y)}}\right) \rightarrow$$

$$\ln[Sw_{(x,y)}(TE) - Bg] = lnPD_{(x,y)} - \frac{TE}{T2_{(x,y)}} (4)$$

c) Non Linear fitting method (NL):
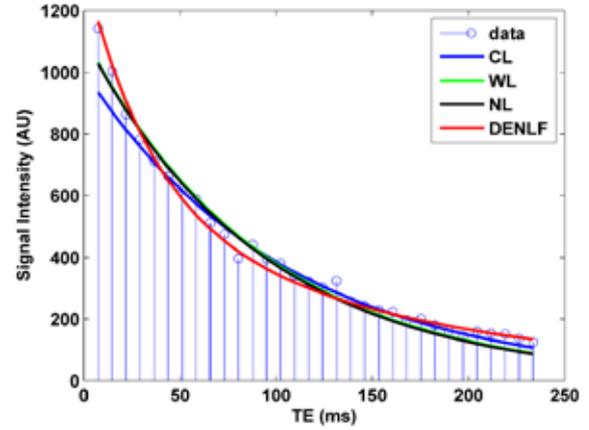In the Non Linear fitting method (NL), all the original echo sig-

nal intensities were directly fitted utilising a mono-exponential decay algorithm for the T2 relaxation decay data (QMRI Utilities-X). The T2 relaxation decay curves were analysed assuming a mono-exponential decay behaviour in the presence of the image background (Bg) which is subtracted from the actual signal data. The signal intensity S of the image of a homogeneous system decays with TE following a mono exponential function [2]. Proton-Density parametric maps $PD_{(x,y)}$ and T2 relaxation time parametric maps $T2_{(x,y)}$ which best fit to the experimental data were calculated by a non-linear single exponential mathematical fit to the equation Eq. (5) on a voxel by voxel basis $_{(x, y)}$ [20-22].

$$S_{(x,y)}(TE) - Bg = PD_{(x,y)}e^{-TE/T2_{(x,y)}} \qquad (5)$$

d) Double Exponential Non Linear fitting method (DENLF):
In the Double Exponential Non Linear method (DENLF), all the original signal intensities were directly fitted assuming the presence of two basic molecular relaxation environments which therefore should be characterised by a double exponential decay curve (QMRI Utilities-X). The T2 relaxation decay curves were analysed assuming a double-exponential decay behaviour in the presence of the image background (Bg) which is subtracted from the actual signal data. In the DENLF regression fitting model, we assume the presence of two molecular environments which should be characterised by a double exponential fitting curve. The first environment is characterised by a short T2 relaxation time (values ranging from 10 ms up to 50 ms) and the second, by a long T2 relaxation time (values
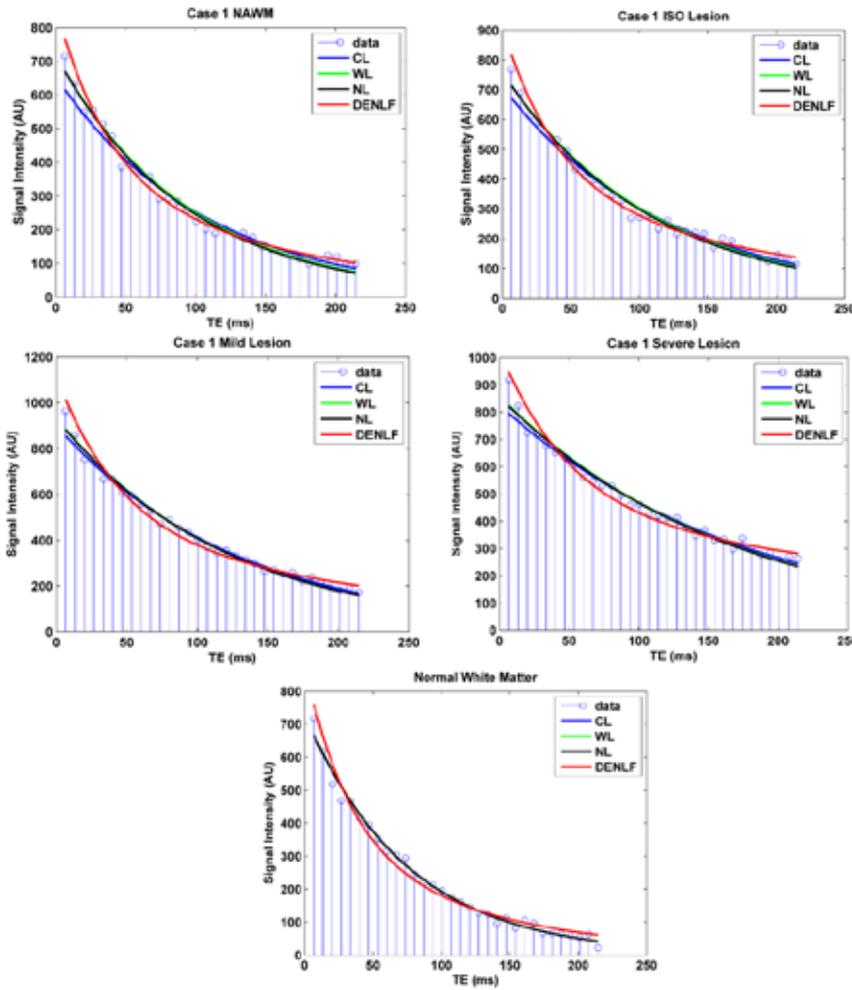
Optimising T2 relaxation measurements on MS patients utilising a multi-component tissue
mimicking phantom and different fitting algorithms in T2 calculations, p. 18-31

VOLUME 4 | ISSUE 2

Fig. 7. *T2 decay curves applying different fitting algorithms (CL, WL, NL, DENLF) on the annotations (ROIs) for each different lesion (NAWM, ISO, Mild, Severe) for human subject case 1 (Fig. 3). A control case with normal white matter is cited for comparison.*

ranging from 60 ms up to the maximum possible, 2000 ms). Four parametric imaging maps namely:

$$PD_{short(x,y)}, PD_{long(x,y)}, T2_{short(x,y)}, T2_{long(x,y)}$$

which best fit to the experimental data were calculated by a non-linear double exponential mathematical fit to the equation Eq. (6) on a voxel by voxel basis (x, y) [20,23].

$$S_{(x,y)}(TE) - Bg = PD_{short(x,y)} e^{\frac{-TE}{T2short(x,y)}} + PD_{long(x,y)} e^{\frac{-TE}{T2long(x,y)}}$$

(6)

In the case of the presence of one molecular environment when the DENLF method is utilised, then simply:

$$PD_{short(x,y)} = PD_{long(x,y)}, \quad T2_{short(x,y)} = T2_{long(x,y)}$$

In both non-linear methods (NL and DENLF), the estimation parameters were computed by fitting the simulated data to the

experimental ones using non-linear curve fitting algorithms which are based on a Levenberg-Marquant methodology, by minimising the metric of x^2.

In all methods (CL, WL NL, DENLF), the background signal (Bg) is obtained from a ROI (BgROI) positioned at an artefact free area outside the actual image and from the latest echo (final echo=32) of the base image stack. It is assumed that image noise, expressed as the SD of the background signal SD (Bg), is evenly distributed in all echo signals or the relative weighted images. For the final image, Gaussian noise calculation SD (Bg) can be expressed by the following equation Eq. (7):

$$SD\ (Bg) = R_f \cdot \sigma S_{32} \qquad (7)$$

Where, the R_f factor (R_f=1.53) is known as the Rayleigh factor and arises when any Gaussian noise (random noise) present on the raw data is centered about zero. σS32 is the measured SD from the actual data obtained from the BgROI positioned on the latest echo (32) signal.

The first echo signal was diminished when compared to the

Optimising T2 relaxation measurements on MS patients utilising a multi-component tissue
mimicking phantom and different fitting algorithms in T2 calculations, p. 18-31

VOLUME 4 | ISSUE 2

HJR

Table 1. Generic T2 relaxation phantom (T2-QMRI phantom): acronyms and chemical composition of phantom test tube vials components

T2-QMRI phantom materials	
Material Acronyms	**Composition**
DDH$_2$0	Double Distilled Water
ACE	Acetone
Gd-DTPA	Gadopentate Dimeglumine
MC	Milk Creams
EWT	Egg White
ECT	Egg Yolk
EOM	1 Egg White and Yolk
W1Y2	1 Egg White and 2 Yolk
W1Y3	1 Egg White and 3 Yolk
W2Y1	2 Egg White and 1 Yolk
W3Y1	3 Egg White and 1 Yolk

Table 2. Generic T2 relaxation phantom: positions of phantom test tube components

Test tubes position			
EUSP1	**EUSP2**	**EUSP3**	**EUSP4**
EUSP5	EUSP6	EUSP7	EUSP8
DDH20	ACE	Gd-DT-PA(15mmol)	Gd-DTPA (10 mmol)
MC1(12%)	MC2(15%)	MC3(15%)	MC4(20%)
MC5(35%)	MC6(35%)	MC7(Soya Milk)	MC8(35%)
Corn Oil	EWT	ECT	EOM
W1Y2	W1Y3	W2Y1	W3Y1

signal of the following echoes. This is mainly due to stimulated echoes or inappropriate refocusing of the 180 pulses. The problem could be avoided by appropriate non-linear correction of the initial short echo signals.

In all methods (CL, WL NL, DENLF), the first echo signal was corrected in order to be used in the final fit. The correction method was based on a nonlinear extrapolation [24] of the expected signal intensity.

For all fitting methods the acceptance criterion applied for the correlation coefficient threshold for the goodness of the fit (r^2) was: $r^2 > 0.8$.

2.5 Phantoms (Data post-processing)

Circular Region of Interest (cROI) of Height 28 (pixels) and Width 28 (pixels), positioned at the center of each test tube, were used for the calculation of mean ROI values. The mean ROI values were obtained by excluding zeros for more accurate calculations, utilising the NordicICE (NordicNeuroLab) software. The Standard Deviations (SDs) from each cROI measurement can be considered as an index of the homogeneity of the T2 measurements assuming homogeneous signal from each test tube sample. The aforementioned cROI calculations

(mean values and SDs) were obtained from each parametric T2 map, which was generated using all four different regression algorithms.

T2-QMRI phantom measurements were repeated five times for a time period of one month in order to estimate T2 value measurements precision. T2 value measurements precision (T2-ROI-CV) expressed by the Coefficient of Variation (CV%) amongst five measurements were obtained for four test tube categories utilising the CL, WL and NL fitting models. The results are presented in **Table 3**. Statistical analysis between the CL, WL and NL fitting methods was performed utilising Bland Altman tests (Bland & Altman, 1986 and 1999). Results are presented in **Fig. 1** and **Fig. 2**.

2.6 Human subjects (Data post-processing)

For each human subject enrolled in this study, one circular region of interest (ROI) was manually defined in the frontal normal white matter of a healthy volunteer and frontal normal appearing white matter (NAWM) of two RRMS patients, case 1 (**Fig. 3**) and case 2 (**Fig. 4**) respectively. In addition, three circular ROIs representing three different types of MS-lesions were identified in the MS-patients' group (case 1 and case 2). All MS-Lesions were firstly identified on conventional T2W images and were classified according to their signal intensity from conventional T1W images by an expert neuroradiologist (EP). More specifically, three focal WM hyperintense lesions were chosen on conventional T2W images and classified according to their signal intensities on conventional T1W images as: 1. Iso-intense to the adjacent WM (ISO) 2. Mildly hypo-intense to the adjacent WM (Mild) and 3. Hypo-intense to the cerebral cortex, with signal intensity similar to that of cerebrospinal

HJR

Optimising T2 relaxation measurements on MS patients utilising a multi-component tissue mimicking phantom and different fitting algorithms in T2 calculations, p. 18-31

VOLUME 4 | ISSUE 2

Table 3. T2 measurements precision CV% (T2-ROI-CV) for a time period of one month				
(CV %) measurements for four test tube categories				
Method	**EUROSPIN**	**Gd-DTPA**	**Milk Creams**	**Raw eggs**
Mean CV-CL	3.28	2.80	15.51	24.94
Mean CV-WL	0.94	0.88	14.94	20.39
Mean CV-NL	0.96	1.49	15.01	20.55
Mean CV-DENLF T2 Short	1.08	0.1	18.95	19.26
Mean CV-DENLF T2 Long	0.76	0.1	27.45	20.84

fluid (severe hypointense=Severe). Once localised on conventional T1W and T2W images, all three MS-lesions ROIs as well as the NAWM ROI were linearly registered and positioned on the (PD to T2)w MESE T2 relaxometry image series and the corresponding T2 maps (**Fig. 3 and Fig. 4**). It is well known that the aforementioned three different types of MS-lesions are characterised by different proportions of demyelination and inflammatory oedema, which are reflected by different short T2 and long T2 values accordingly [25].

Results

3.1 Phantoms

The generated T2 maps from all four different fitting algorithms are presented in **Fig. 5**. An example of the numerical fitting graphical results for a particular pixel positioned on the milk cream tube (MC5 35%) is presented in **Fig. 6**, where the DENLF method reveals numerical data fitting with better accuracy than all the other methods. Finally, by concerning the correlation coefficient (r^2) as a metric for the goodness of each fit, the WL and NL methods revealed an r^2 equal to 0.9978 and 0.9980 respectively. CL method revealed an r^2 equal to 0.9850. DENLF method revealed an r^2 equal to 0.9992.

In an attempt to assess the homogeneity of T2 measurements, in reference to the previously discussed circular measurement ROIs (cROI), the mean Standard Deviations (SDs) obtained by the WL and NL for all EUROSPIN test tube vials were almost the same, namely 0.6816, 0.6884 respectively. The CL method led to larger mean SD (1.806) than the other methods for the same test tubes. In the DENLF method, the mean SD obtained by T2 short component was 0.2843 and 1.2357 for T2 long component.

T2 values of all EUROSPIN gel test tubes were in agreement with their nominal values (accuracy <5%) [15-17]. EUROSPIN gel test objects and Gd-DTPA hydatic solutions were characterised by single T2 values. Milk creams and raw eggs were characterised by double T2 values. Concerning CV% measurements

(**Table 3**), NL method reveals almost similar mean T2-ROI-CV values as compared to WL method. CL method reveals the worst mean T2-ROI-CV results (**Table 3**).

EUROSPIN test objects and Gd-DTPA solutions (**Table 3**) reveal low mean T2-ROI-CV values (<3%) independent from the fitting model. However, milk creams and raw eggs due to their natural spoilage revealed higher mean T2-ROI-CV values (<25%).

Bland-Altman plots were created for all EUROSPIN test objects (**Fig. 1**) and milk creams (**Fig. 2**), to compare the different measurement techniques. In the selected Bland-Altman method the mean percent T2 value differences between the two techniques are plotted against their mean measured T2 values.

In the study of EUROSPIN test objects, the comparison between WL and NL reveal a very low mean percent T2 value difference (0.95%) whereas the comparison between WL and CL reveal a mean percent T2 value difference of 17%. NL and CL showed a mean percent T2 value difference of 16.1% (**Fig. 1**). The same graphical plots were generated for milk creams (**Fig. 2**) where WL and NL reveal a very low mean percent T2 value difference (0.85%). CL and WL show a mean percent T2 value difference of 1.9%. CL and NL showed a mean percent T2 value difference of 2.8%.

3.2 Human subjects

From the aforecited correlation coefficients, the CL method revealed a lower r2 from all our in-house algorithms (**Table 4**). That means that the estimated curve as assessed by the CL method is less related to the experimental data, where on the other hand WL, NL and DENLF are more correlated and thus more reliable (**Table 4, Figs. 7, 8.**). T2 decay curves applying different fitting algorithms (CL, WL, NL, DENLF) on the annotations (ROIs) for each different lesion (NAWM, ISO, Mild, Severe) for human subject case 1 and human subject case 2 are presented in **Fig. 7** and **Fig. 8** respectively. In either human subject case, a T2 decay curve of a control human subject case

Optimising T2 relaxation measurements on MS patients utilising a multi-component tissue mimicking phantom and different fitting algorithms in T2 calculations, p. 18-31

VOLUME 4 | ISSUE 2

HJR

Table 4. Results of the goodness of the fit r2 and the calculated T2 values (ms) for each different in-house algorithms (CL, WL, NL, DENLF), for three different lesions (ISO, Mild, Severe) assigned on two different patients (Case 1, Case 2) and a normal subject (Normal)

CASE 1

Method	r^2	NAWM	r^2	ISO	r^2	Mild	r^2	Severe
CL	0.9899	105	0.9905	117	0.9938	128	0.9892	189
WL	0.9923	95	0.9920	109	0.9945	121	0.9899	179
NL	0.9927	93	0.9924	107	0.9945	121	0.9899	179
DENLF-T2 short	0.9928	37	0.9927	40	0.9950	44	0.9901	54
DENLF-T2 long	0.9928	167	0.9927	207	0.9950	248	0.9901	576

CASE 2

Method	r^2	NAWM	r^2	ISO	r^2	Mild	r^2	Severe
CL	0.9947	98	0.9953	104	0.9889	132	0.9821	203
WL	0.9954	93	0.9955	101	0.9902	123	0.9837	187
NL	0.9955	92	0.9956	100	0.9902	123	0.9837	187
DENLF-T2 short	0.9957	37	0.9956	40	0.9915	42	0.9909	53
DENLF-T2 long	0.9957	157	0.9957	176	0.9915	258	0.9909	691

NORMAL

Method	r^2	T2 meas
CL	0.9956	75
WL	0.9956	75
NL	0.9956	75
DENLF-T2 short	0.9959	30
DENLF-T2 long	0.9959	119

with normal white matter is presented for comparison (**Table 4, Figs. 7, 8**).

DENLF method provides valuable extra information by estimating short T2 and long T2 value components simultaneously (**Table 4, Figs. 3, 4, 7, 8**). Therefore, two distinct different molecular environments from a single set of TE values could be extracted. This is very profitable and of paramount importance considering that in the human brain most of the normal tissues and pathologies are described by double exponential (short and long) T2 values.

Discussion

4.1 Phantoms
In this work four different regression fitting algorithms were applied for optimal measurements of T2 relaxation times in tissue mimicking phantoms.

The Conventional Linear method (CL)

The CL method is considered as a fast but not accurate means for T2 measurements. The measured T2 values as assessed by the CL method for the EUROSPIN test tubes are not in concordance to the nominal T2 measurements. The CL method for the calculation of T2 values of Gd-DTPA, ACE and DDH20 proved inefficient due to the low r^2 value ($r^2 < 0.8$). The main drawback of this method is that the algorithm used for T2 and PD calculations is based upon global minimum variance estimators without any T2 decay signal weighting, which may cause lack of accuracy for the final T2 calculations.

The Weighted Linear method (WL)

This weighted algorithm, as presented in this study, is an excellent means for T2 measurements. The measured T2 values as assessed by the WL method for the EUROSPIN test tubes are in concordance to the nominal T2 measurements. The same results apply for the NL method, having as a big advantage
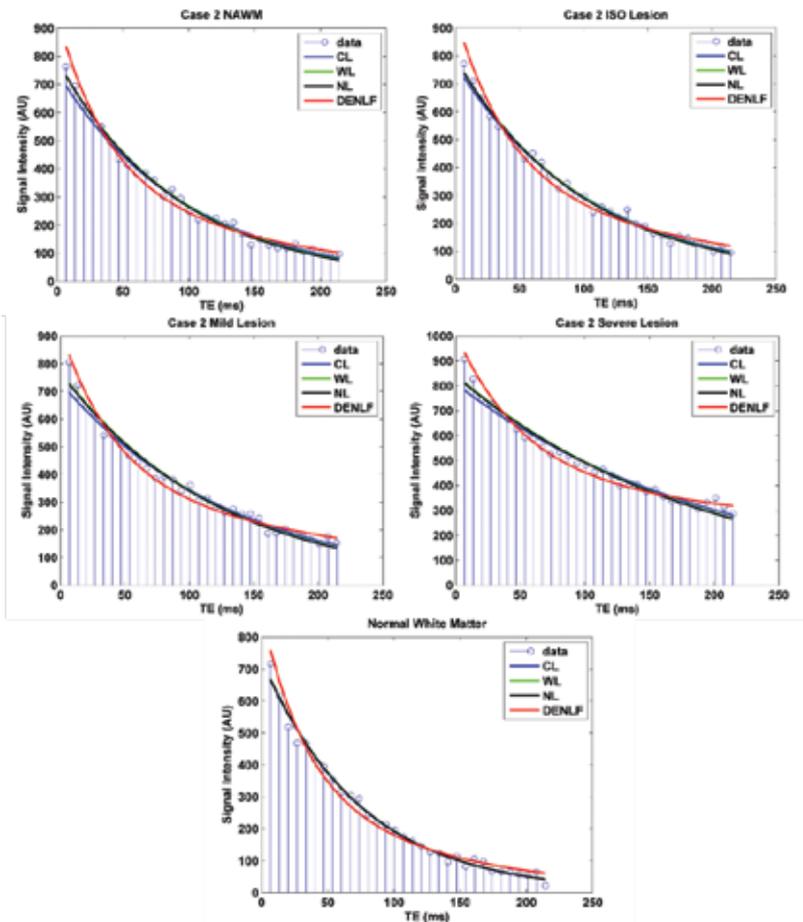
HJR

Optimising T2 relaxation measurements on MS patients utilising a multi-component tissue
mimicking phantom and different fitting algorithms in T2 calculations, p. 18-31

VOLUME 4 | ISSUE 2

Fig. 8. *T2 decay curves applying different fitting algorithms (CL, WL, NL, DENLF) on the annotations (ROIs) for each different lesion (NAWM, ISO, Mild, Severe) for human subject case 2 (Fig. 4). A control case with normal white matter is cited for comparison.*

the fast computation time, since it is using a linear weighted regression analysis fitting factor as stated in equations Eq. (3) and Eq. (4). In WL the T2 decay curves are weighted prior to the final linear fit with weighting factors obtained from Rayleigh distributions for each sequence of 32 echoes. Fitting methods that use noise-corrected functions lead to better T2 measurement accuracy.

The Non-Linear method (NL)

The non-linear method based on a single exponential behaviour is generally considered from the present literature as the standard method for T2 measurements. The estimated T2 measurements for the EUROSPIN test tubes are in concordance with their nominal values. In NL a nonlinear fit is performed minimising the sum of quadratic distance of the noise-free model to S(TE) with no logarithm transformation. The NL method is based on the inherent non-linear character of the fitting model.

The Double Exponential Non-Linear method (DENLF)

DENLF method revealed a better accuracy for all the materials used in this study, especially in those consisted of two (short

and long) molecular environments (**Fig. 6**). In this method, a double exponential fit is performed minimising the sum of quadratic distance of the noise-free model to S(TE) with no logarithmic transformation. The short T2 component present on the milk cream phantoms can be associated with the myelin bound water fraction (value near 30 ms for normal human subject) [4, 6]. This in turn can serve as an important diagnostic means for quantifying demyelination processes in brain MRI. On the other hand, the long T2 component can be associated with the extracellular space (water reservoirs). Consequently, this double-exponential behaviour of T2 decay curves in brain white matter provides a significant tool to monitor the myelin water component in MS lesion and to monitor the expansion of the extracellular space which can be revealed in long T2 component [7].

Comparing all the fitting methods

In reference to the correlation coefficient (for the particular numeral fitting of **Fig. 6**), the CL method revealed a lower r2 than all the other methods. Thus, the estimated curve as assessed by the CL method is less related to the experimental data, where on the other hand WL, NL and DENLF are more

Optimising T2 relaxation measurements on MS patients utilising a multi-component tissue
mimicking phantom and different fitting algorithms in T2 calculations, p. 18-31

VOLUME 4 | ISSUE 2

correlated and thus more reliable. Comparing the four different numerical fitting methods regarding the Standard Deviation, for all EUROSPIN test tubes, the mean SD obtained by the CL method is higher compared to WL, NL and DENLF. This in turn determines that the parametric T2 maps extracted with those algorithms have higher homogeneity and consequently better accuracy and reliability in T2 calculations.

In Bland-Altman plots for both EUROSPIN test tubes and milk creams objects, the WL and NL methods revealed a very low mean percent T2 value differences (0.95% and 0.85% respectively), which means that the two methods are almost similar, as it can be observed by their results (**Figs. 5, 6**). WL method has an important advantage of being significantly faster as compared to the NL method.

4.2 Human Subjects

Long T2 components like cerebrospinal fluid could be measured accurately when appropriate multi echo trains are used. The T2 measurement accuracy depends upon the number of echoes and the inter-echo interval of the echo signals. Initially it is obvious that in order to accurately measure T2 values we need as many echo signals (TEs) to cover a time space equivalent at least to the T2 value. This is not generally the case. We can measure a T2 value utilising short TE intervals which is linearly related to the actual long T2 value of the tissue in question [26, 27]. The use of short echo signals is always a benefit to relaxometric procedures because we are measuring signals of the highest possible SNR values.

Multiple sclerosis (MS) is a common autoimmune disorder of the Central Nervous System (CNS) characterised by inflammatory demyelination and secondary axonal degeneration. About 85% of patients are affected by relapsing/remitting MS (RRMS) and characterised by recurrent attacks of neurologic dysfunction. Due to its high sensitivity in identifying free water within the normally myelinated white matter, MRI and particularly T2 sequences have become the ideal imaging modality for the detection of cerebral white matter diseases. Whereas, conventional MRI reveals focal WM lesions in all patients with RRMS fails to detect the microstructural damage revealed by quantitative MRI techniques in otherwise normal WM areas, so called normal appearing white matter (NAWM) [25]. Previous studies by using multi-echo T2 relaxation sequences have shown that there is decreased myelin water in the lesions, as well as NAWM, for patients with RRMS relative to normal controls, while there is, also, greater loss of myelin integrity with more advanced disease [28-32]. Unfortunately, these studies suffer from prolonged scanning times [12]. In recent studies, a fast

triple component multi-echo sequence is used for the quantification of MS lesions [26, 27].

According to the current literature, T2 relaxation times in normal brain follow a multi-compartment or multi-exponential model of at least two or more independent T2 parameter molecular environments [4, 33]. This could be considered the basis of MR relaxometry in brain tissues. Bi-exponential fitting has proven an essential tool for soft tissue relaxometry measurements.

In our study, a two compartment model is suggested. In this case a short (10<T2<50 ms) and a long (T2>60 ms). T2 components reflect the myelin water and both the intra-extra cellular water and the free water environments respectively.

Several multi-echo-spin-echo multi-compartment quantitative sequence schemes exist in the literature. These include: (a): 2D single/multi slice multi-echo schemes with spectral T2 analysis post-processing algorithms based on Laplace transforms [4], (b): 2D and 3D multi slice simultaneous GRAdient and Spin Echo (GRASE) methods [34], (c): T2 preparation multi slice methods [35], and (d): whole brain 3D multicomponent driven-equilibrium single-pulse observation time (mcDESPOT) methods for simultaneous multi-compartment T1 and T2 measurements [36, 37]. All sequences have specific advantages and disadvantages in relation to the accuracy and the sensitivity of T2 measurements for which they were designed [12].

The number, echo spacing and covering range of the echoes are always crucial factors for the sensitivity of the final T2 measurement. Amongst all multi-echo spin echo sequences the methods proposed by MacKay et al [4] and its variants are those which are still considered as reference methodologies in T2 relaxometry nowadays. They all use 32 echoes as their basic characteristic for brain tissue T2 measurements. The main drawbacks are the single slice acquisitions, the elevated echo spacing (10 ms) and the long examination times (25 mins) in most of the sequences. 3D GRASE sequences [34] offer the advantage of total brain anatomical coverage. However, they are using long examination times for clinical protocols and extremely low TR (1000 ms) for accurate brain tissue T2 relaxometry. The inherent drawback on these sequences is the strong signal T2* dependence on the peripheral K-space lines. T2-prep sequences [35] offer the advantage of 2D multi-slice and in some cases total brain anatomical coverage. They possess the ultimate advantage of being insensitive to cumulative errors of stimulated echoes due to the T2-prep rationale. They are also using short and variable echo spacing. However, they possess the disadvantages of quite long examination times (15 mins) and a limited number of echoes (12 echoes).

HJR

Optimising T2 relaxation measurements on MS patients utilising a multi-component tissue
mimicking phantom and different fitting algorithms in T2 calculations, p. 18-31

VOLUME 4 | ISSUE 2

mcDESPOT sequences [36, 37] do offer an alternative indirect way to measure T1 and T2 simultaneously. These sequences possess the advantage of total brain anatomical coverage and short variable echo spacing. However, they still use long examination times (30 mins) and an extremely small number of the echoes, only three echoes, for measuring T2. The mcDESPOT is indeed a promising alternative in indirect T2 relaxometry measurements, but a clinical study comparing this type of sequences with conventional MESE sequences on the same human subjects is certainly missing from the current literature.

For the purposes of the clinical part of this study, an optimised MESE sequence is proposed. The double exponential fitting model, as presented and utilised in the phantom studies, proved to be a fast (3.5 mins) and accurate means for two compartments simultaneous T2 measurements ranging from 10 up to 300 ms applied in clinical studies [37]. The optimised 2D MESE sequence described above was chosen as the best alternative,

for the fulfillment of the purposes of the clinical part of this study, as compared to the sequences existed in the literature.

In conclusion, amongst the four different regression fitting algorithms, the DENLF algorithm seemed to be an excellent means for optimised T2 relaxation measurements in brain tissue mimicking phantoms. In addition, the DENLF algorithm, when applied in healthy control subjects and RRMS patients, showed excellent results regarding T2 relaxometry measurements, which in turn may improve the final MR imaging diagnostic value. This is a proof of concept approach for an initial clinical evaluation and it is described in detail on the technical part. The extended clinical evaluation is presented on two separate studies using the proposed algorithm [26, 27].**R**

Conflict of interest
The authors declared no conflicts of interest.

References

1. Jones C, MacKay A, Rutt B. Bi-exponential T2 Decay in Dairy Cream Phantoms. *Magn Reson Imaging* 1998; 16: 83-85.

2. Carneiro AAO, Vilela GR, de Araujo DB, et al. MRI Relaxometry: Methods and Applications. *Braz J Phys* 2006; 36: 9-15.

3. Whittal KP, MacKay AL, Li DK. Are mono-exponential Fits to a Few Echoes Sufficient to determine T2 Relaxation for in vivo human brain? *Magn Reson Med* 1999; 41: 1255-1257.

4. MacKay A, Whittall K, Adler J, et al. In vivo visualization of myelin water in brain by magnetic resonance. *Magn Reson Med* 1994; 31: 673-677.

5. Liu H, Yang Y, Xia Y, et al. Aging of cerebral white matter. *Ageing Res Rev* 2017; 34: 64-76.

6. Kumar R, Delshad S, Woo MA, et al. Age-Related regional brain T2-Relaxation changes in healthy adults. *J Magn Reson Imaging* 2012; 35(2): 300-308.

7. Levesque IR, Pike GB. Characterizing healthy and diseased white matter using quantitative magnetization transfer and multicomponent T2 relaxometry: an unified view via a four-pool model. *Magn Reson Med* 2009; 62: 1487-1496.

8. Kumar R, Delshad S, Macey PM, et al. Development of T2-relaxation values in regional brain sites during adolescence. *Magn Reson Imaging* 2011; 29(2): 185-193.

9. Grydeland H, Walhowd KB, Tamnes CK, et al. Intracor-tical myelin links with performance variability across the human lifespan: results from t1- and t2- weighted mri myelin mapping and diffusion tensor imaging. *J Neurosci* 2013; 33(47): 18618 -18630.

10. Saito N, Sakai O, Ozonoff A, et al. Relaxo-volumetric multispectral quantitative magnetic resonance imaging of the brain over the human lifespan: global and regional aging patterns. *Magn Reson Imaging* 2009; 27: 895-906.

11. Badvem C, Yu A, Rogers M, et al. Simultaneous T1 and T2 brain relaxometry in asymptomatic volunteers using magnetic resonance fingerprinting. *Tomography* 2015; 1(2): 136-144.

12. Alonso-Ortiz E, Levesque IR, Pike GB. MRI-Based myelin water imaging: a technical review. *Magn Reson Med* 2015; 73: 70-81.

13. Billiet T, Vandenbulcke M, Madler B, et al. Age-related microstructural differences quantified using myelin water imaging and advanced diffusion MRI. *Neurobiol Aging* 2015; 36: 2107-2121.

14. Laule C, Vavasour IM, Madler B, et al. MR Evidence of long T2 water in pathological white matter. *J Magn Reson Imaging* 2007; 26: 1117-1121.

15. Lerski RA, De Certaines JD. Performance assessment and quality control in MRI by Eurospin test objects and protocols. *J Magn Reson Imaging* 1993; 11(6): 817-833.

Optimising T2 relaxation measurements on MS patients utilising a multi-component tissue mimicking phantom and different fitting algorithms in T2 calculations, p. 18-31

VOLUME 4 | ISSUE 2

HJR

16. Lerski RA, McRobbie DW, Straughan K, et al. Multi-center trial with protocols and prototype test objects for the assessment of MRI equipment. EEC Concerted Research Project. *Magn Reson Imaging* 1998: 6(2): 201-214.

17. Price PR, Axel L, Morgan T, et al. Quality assurance methods and phantoms for magnetic resonance imaging: report of AAPM nuclear magnetic resonance Task Group No. 1. *Med Phys* 1990: 17(2): 287-295.

18. Fransson A, Ericsson A, Jung B, et al. Properties of the PHase-Alternating Phase-Shift (PHAPS) multiple spin-echo protocol in MRI: A study of the effects of imperfect RF pulses. *Magn Reson Imaging* 1993; 11: 771-784.

19. Maris TG, Damilakis J, Sideri L, et al. Assessment of the skeletal status by MR relaxometry techniques of the lumbar spine: comparison with dual X-ray absorptiometry. *Eur J Radiol* 2004; 50: 245-256.

20. Marquardt DW. An algorithm for least squares estimation of non-linear parameters. *J Soc Industr Appl Math* 1963; 2: 431-441.

21. Draper NR, Smith H. Applied regression analysis. Wiley, New York, 1966, pp 272-274.

22. Breger RK, Rimm AA, Fischer ME, et al. T1 and T2 measurements on a 1.5-T commercial MR Imager. *Radiology* 1989; 171: 273-276.

23. Vasilescu V, Katona E, Simplaceanu V, et al. Water compartments in the myelinated nerve III. Pulsed NMR result. *Experientia* 1978; 34 (11): 1443-1444.

24. Lebel RM, Wilman AH. Transverse relaxometry with stimulated echo compensation. *Magn Reson Med* 2010; 64: 1005-1014.

25. Moll NM, Rietsch AM, Thomas S, et al. Multiple sclerosis normal-appearing white matter: pathology-imaging correlations. *Ann Neurol* 2011; 70(5): 764-773.

26. Kavroulakis E, Simos GP, Kalaitzakis, G et al. Myelin content changes in probable alzheimer's disease and mild cognitive impairment: associations with age and severity of neuropsychiatric impairment. *J Magn Reson Imaging* 2017; 47(5): 1359-1372.

27. Papadaki E, Kavroulakis E, Kalaitzakis G, et al. Age Related Deep White Matter Changes in Myelin and Water Content: A T2 Relaxomety study. *J Magn Reson Imaging* 2019 doi: 10.1002/jmri.26707. [Epub ahead of print].

28. Oh J, Han ET, Lee MC, et al. Multislice brain myelin water fractions at 3T in multiple sclerosis. *J Neuroimaging* 2007; 17: 156-163.

29. Tozer DJ, Davies GR, Altmann DR, et al. Correlation of apparent myelin measures obtained in multiple sclerosis patients and controls from magnetization transfer and multicompartmental T2 analysis. *Magn Reson Med* 2005; 53: 1415-1422.

30. Rumbach L, Armspach JP, Gounot D, et al. Nuclear magnetic resonance T2 relaxation times in multiple sclerosis. J Neurol Sci 1991; 104: 176-181.

31. Kitzler HH, Su J, Zeineh M, et al. Deficient MWF mapping in multiple sclerosis using 3D whole brain multi-component relaxation MRI. *Neuroimage* 2012; 59(3): 2670-2677.

32. Kolind S, Matthews L, Johansen-Berg H, et al. Myelin water imaging reflects clinical variability in multiple sclerosis. *Neuroimage* 2012; 60: 264-270.

33. Vavasour IM, Whittall KP, Li DKB, et al. Different magnetization transfer effects exhibited by the short and long T2 components inhuman brain. *Magn Reson Med* 2000; 44: 860-866.

34. Oshio K, Feinberg DA. GRASE (Gradient-and Spin-Echo) imaging: a novel fast MRI technique. *Magn Reson Med* 1991; 20: 344-349.

35. Nguyen TD, Wisnieff C, Cooper MA, et al. T2 prep three-dimensional spiral imaging with efficient whole brain coverage for myelin water quantification at 1.5 tesla. *Magn Reson Med* 2012; 67: 614-621.

36. Deoni SCL, Rutt BK, Peters TM. Rapid combined T1 and T2 mapping using gradient recalled acquisition in the steady state. *Magn Reson Med* 2003; 49: 515-526.

37. Deoni SCL, Rutt BK, Arun T, et al. Gleaning multicomponent T1 and T2 information from steady-state imaging data. *Magn Reson Med* 2008; 60: 1372-1387.